IN-76-CR
88660
p 31

GLASS FORMABILITY OF HIGH T_C BI-SR-CA-CU-O SUPERCONDUCTORS

Final Report

NASA Grant NAG8-152

by

Dr. William F. Kaukler

William F. Kaukler

Department of Chemistry,

The University of Alabama in Huntsville,

Huntsville, Alabama 35899

May 7,1992

Abstract

A number of compositions of ceramic oxide high Tc superconductors were evaluated for their glass formation ability by means of rapid thermal analysis during quenching, optical and electron microscopy of the quenched samples, and with subsequent DSC measurements. Correlations between experimental measurements and the methodical composition changes identified the formulations of superconductors that can easily form glass. The superconducting material was first formed as a glass, then with subsequent devitrification it was formed into bulk crystalline superconductor by a series of processing methods.

Discipline: Glass Science

Key Words: Crystallization, Glass, Glass-ceramics, Nucleation, Thermal Analysis, Superconductivity

Introduction

The revolutionary and historic advances in high temperature superconductivity starting with La-Sr-CuO[1] and followed by the discovery of the 123 Y-Ba-CuO[2], Bi-Sr-Ca-CuO[3], and Th-Ba-CuO[4] oxide ceramics have become widely known. It has been shown that the Bi-Sr-Ca-CuO (or BSCCO) is a reasonably good glass forming system[5,6,7]. It was immediately recognized that if superconducting materials could be melted, formed into glass, and crystallized, the possibility existed for having a wide range of processing methods to shape the superconductor into monolithic shapes, filaments, and wires[8,9].

The purpose of this study was to examine the critical cooling rates and glass formation ability for glass forming compositions of oxide high temperature superconductor materials. From the onset, it was known that modifications to the batch compositions would be required in order to enhance glass formation to the extent required to form bulk materials. The goal was to produce glass precursor material from which high superconducting critical transition temperature (T_c) crystalline glass-ceramics could be produced.

Besides the obvious advantages of producing useful products from glass preforms, it is believed that the crystalline grain boundaries formed by in situ crystallization from the glass are fundamentally different from the crystal grain boundaries produced by the solid state diffusion processes. Interesting research into the current-limiting interface could be performed from detailed studies of superconducting glass-ceramics.

Preparation of two papers for publication of the results is under way. One, the fist to submit, regards the Glass Formability based on cooling rates from quenches. It is in this paper that evaluation of the various recipes will be summarized. The second paper will tie in with the first and will build upon it. It is in the second paper where the major results from thermal analysis and magnetic studies will be assessed.

The efforts in this project are shared by two others; Dr. Edwin Ethridge, of MSFC, NASA, the originator of concept and Co-investigator, and Terry Rolin, our part-time graduate research assistant who performed some analysis, found references, shared his expertise and is continuing the project in the form of a PhD Thesis.

Experimental Procedure

The plan of the investigation was to evaluate the glass forming ability with emphasis on the compositional dependence of glass formation in the BSCCO system. The goal was to quantify the glass formation ability of the materials to find the best glass forming compositions. Glass formation data was obtained from quenching experiments, thermal analysis, and microstructural analysis studies of the materials.

The six compositions from the system Bi-Sr-Ca-Cu-O examined in this study are shown in Table 1 and are plotted on a triaxial diagram in Fig 1 with Bi_2O_3 and CuO on two corners and the total of CaO plus SrO at the third corner. A literature search indicated 2112 and 4334 as prospective good glass forming candidates (Komatsu et al, 1988[7],; Tatsumiago et al, 1989[8]; and Bhargava et al, 1989[6]). The other compositions including, 2212, 2223, 2234, and 2245 were selected based on results of the literature search and preliminary results from this work. It should be noted that the batch proportions 2112, 4334, and 2212 represent the stoichiometric proportions of the three known superconducting phases in this system.

TABLE 1 **Nominal Compositions (mole fraction)**

Sample	(Bi2O3)/2	SrO	CaO	CuO
2112	.33	.165	.165	.330
4334	.286	.21	.21	.286
2212	.286	.286	.14	.286
2223	.222	.222	.222	.333
2234	.182	.182	.273	.364
2245	.154	.154	.308	.385

Glass batches were produced using calcined reagent grade oxides and carbonates. The powders were calcined at temperatures greater than 500°C and stored in desiccators. The appropriate compound for each constituent was weighed, the batch was mixed, charged into platinum crucibles, and melted in a SiC furnace in air at around 1250 to 1300 °C for about 15 to 20 minutes but for no more than 30 minutes. The molten material was very fluid for all the batches tested. To ensure that the melt was homogeneous with the constituents fully dissolved and mixed the crucible containing the melt was briefly removed from the furnace and swirled to mix the liquid and then returned to the furnace. Splat quenches were performed by pouring the melt onto a graphite plate and pressing with another graphite plate, both initially at room temperature. Spacers of various thicknesses were used to produce foils of different thicknesses resulting in a range of cooling rates. The foil shaped samples were examined and a subjective qualitative evaluation of the extent of glass formation was made from observations of the fracture surfaces of the quenched samples using optical and scanning electron microscopy.

For some quench runs the actual cooling rate was measured by inserting a fine wire (0.005 in. diameter) type S thermocouple into the melt immediately upon pouring and prior to pressing of the graphite plates. A computer controlled rapid thermal analysis system permitted the high resolution and high data rate required to directly obtain the cooling curve data of the splat quenches and the subsequent determination of the cooling rates of the splatted melts. The temperature data in the form of a mV signal from the thermocouple was collected at 10 millisecond intervals for 10 seconds via Keithly System 500 Data Acquisition and an MS-DOS PC-AT type clone computer. Unexpected problems were encountered with the thermocouple measurements. Wildly fluctuating mV values representing temperatures from below zero to several hundred degrees above the starting melt temperature were recorded. This is attributed to electrical conduction in the melt and thermoelectric effects between the thermocouple wires and the melt. It was found that an insulating layer of lacquer applied to the thermocouple usually prevented this electrical interaction between the melt and the thermocouple elements. The lacquer immediately burnt on contact with the hot glass and although not every measurement was successful, useful data was obtained in many cases. Cooling rates ranging from 50 to 4000 °C/sec were measured.

The rapid thermal analysis apparatus (RTAA) and the high temperature strip heater furnace designed at MSFC were used to study glass formation in reluctant glass forming systems. The RTAA consists of an ellipsoidal furnace that has been automated for computer control and data acquisition, see

Fig 2. Repeated heating and quenching can be accomplished under unattended software control with thermal data being saved to hard disk in Lotus 123 compatible files.

The strip heater was utilized for sample preparation for use in the RTAA. Pieces of pre-melted glass were placed onto the Pt strip heater foil. The voltage was ramped up until melting was observed. A prefabricated thermocouple connected to a thermocouple meter was inserted into the molten material to produce a superconducting coating on the thermocouple bead.

Differential scanning calorimetry and differential thermal analysis are very useful methods for the investigation of nucleation kinetics. It was recognized that our group needed a state of the art system for these studies and to correlate thermal data obtained with known methods with that obtained with the RTTA. At the beginning of the study a differential scanning calorimeter was ordered. Due to the long procurement time it did not arrive until nearly one year after the scheduled completion of the study. In the interim we were able to utilize an Omnitherm STA 1500 DTA/TG at UAH.

The research was focused on the processing of compositions that could form the highest temperature superconducting phases. It was learned that compositions around the stoichiometric high Tc phase could be quenched to glass quite easily. The glass could then be transformed into the high Tc phase with appropriate thermal annealing. Glass batches of a number of BSCCO compositions were prepared. The glasses were crystallized and annealed in an oxygen-containing atmosphere in the temperature range of 775 to 825^{o}C for extended times (1 to 48 hours) to develop the high temperature superconducting phases. Superconductivity properties of nominally 50 mg size samples were determined with a Quantum Design Magnetic Measurement System SQUID magnetometer using standard procedures.

Results and Discussion

Fig 3 shows a collection of optical micrographs of glass samples from four selected compositions in the as-quenched state prepared by splat quenching between graphite plates. Each show the degree of glass formation. The uniform areas of material without structural detail are amorphous regions. Some small crystallites are frequently found within the amorphous continuous phase, but represent only a small fraction of the total bulk material. Glass formation was confirmed with x-ray diffraction, microscopy, and thermal analysis. The best glasses were formed from the 2112 and 4334 compositions.

The 2112 batch is the easiest glass former of the set and appears to have the lowest melting temperature. Glass formation was also found over a wide range of quench rates with both 2112 and 4334. Glass formation is favored by compositions closer to the Bi_2O_3 corner of the diagram (Fig 1) as indicated from published results with 2.7,1,1,2 and our results with 2112. The two compositions (4334 and 2212) have the same ratios of Bi_2O_3:CuO:SrO(CaO) and therefore appear on the same point in Fig 1. The 4334 batch has more CaO (less SrO) and is a better glass former. It is also a better high Tc glass-ceramic. This indicates that extra CaO both enhances glass formation and high Tc properties in the resulting glass-ceramic.

Glass formation ability decreased as the percentage of Bi_2O_3 decreased and the series of batches 2223, 2234, and 2245 were relatively poor glass formers. Even splatting to very thin foils did not produce glasses from these compositions. The latter two melted with difficulty and were the poorest glass formers.

Estimates were made of the critical cooling rates for glass formation based on a set of quenches covering a wide range of quench rates. Critical cooling rates for formation were measured as low as 200 ^{o}C/sec for the good glass formers and as high as 2000 ^{o}C/sec for the poor glass formers. Typical cooling curves produced by rapid cooling between graphite plates are shown in Figs. 4, 5, and 6. Quench rates from 50 to 4000 degrees per second could be obtained. Analysis of the data was performed using a

spreadsheet to permit plotting the cooling curves and their derivatives to determine cooling rates. Most of the quenches were in the range from 60 to 800 degrees per second. Table 2 shows qualitative data on the extent of glass formation, sample thicknesses, and quench rates for some of experiments.

In several hundred quenching experiments with the automated rapid thermal analyzer it was shown that many of the compositions from the BSCCO system are glass formers without the addition of glass forming additives. The RTAA was also used to quench samples to determine critical cooling rates. Fig 7A and 8A show quenching and re-heating curves respectively for 2112. Whereas Figs 7B and 8B show the calculated derivative of the cooling (heating) curve, which is the quenching or heating rate.

Rapid thermal analyzer quenching data from sample 2112 using the automated rapid thermal analyzer. Fig. 7a is the temperature data where as Fig. 7b is the derivative of the temperature data calibrated in deg. C per sec being equivalent to an uncalibrated plot of heat capacity. One can see an inflection in the cooling curve at about 780 ^{o}C. This is an anomalous heat capacity effect at glass transition. Before the glass transition the cooling rate is 275 ^{o}C/sec and after the glass transition the cooling rate is 325 ^{o}C/sec. This indicates that the heat capacity of the undercooled liquid is more than the heat capacity of the glass.

Re-heating data from the rapid thermal analyzer for a glass sample of 2112 (8a) and the calculated delta temperature data (8b). The plot of cooling rate vs. time (temperature) is very similar to conventional DTA data. A peak indicating an increased heating rate corresponds to an exotherm (i.e. the glass crystallization peak at about 520 C. Endotherms are indicated by a decrease in the heating rate (i.e. glass transition at 460 ^{o}C). Melting begins with an endotherm at about 760 ^{o}C.

Traditional theoretical nucleation and crystal growth calculations were programmed with MathCAD by Dr. Ethridge[13]. The calculations are most dependent on viscosity data for the undercooled liquid. Utilizing viscosity data for composition close to 2112, calculations of the crystallization rate were performed[13].

The classical calculations predicted glass formation in agreement with the splat quenching and RTAA experiments. The crystallization behavior of these glasses is similar to the LBAN class of fluoride glass. A wealth of information exists for the formation of glass fibers and bulk preforms of the low viscosity fluorides. The same processing methods might be utilized to produce useful shapes from the high temperature superconductors.

Annealing of the glassy specimens is required to recrystallize the specimen into a useful superconducting material. Broken, bulk pieces were annealed in air at 800 ^{o}C for 20 hours followed by soaking at 825 ^{o}C for 86 hours in Oxygen. Since 2112 showed signs of melting at the above conditions, the annealing was performed at 775 ^{o}C in air for 20 hours and then in oxygen for 72 hours. Some measurements of annealed specimens have been made at UAH with the Quantum Design SQUID Magnetometer, a JEOL SEM, and with a Norelco X-ray Diffraction Analyzer. Optical microscopy was performed on polished sections of both splatted and annealed specimens. Based on these observations, it appears two main phases are forming in these materials after annealing. Depending on the batch composition, the glassy splats show varying small volume fractions of crystalline inclusions, as may be seen in Fig. 3. All splats for all batches showed at least a tiny fraction of crystalline phase. Some, like 2212 and 4334 showed significant quantities of crystalline phases. These phases lose their identity after annealing. With 4334 splats, the crystalline, acicular, needle-like precipitates were found emanating inward from the quench surfaces indicating a susceptibility for surface heterogeneous nucleation.

TABLE 2

Composition	Date	Thickness (in mm)	Quench Rate (^{o}C/sec)	Glass Formation (vp,p,g,vg)
2112	5/90	0.55		glass
2112	5/90	0.58		glass
2112	8/90	0.66		vvg
2112	5/90	0.67		glass
2112	8/90	0.82		vvg
2112	8/90	1.23	900	glass
2112	8/90	3.87		vp
4334	6/90	0.49		glass
4334	8/90	0.55		vvg
4334	6/90	1.44		vvg
4334	8/90	2.12		p
4334	6/90	3.22		p
2212	NA	thin	4000	glass
2212	NA	thick	75	unkwn
2212	8/90.24	0.2+	300	NA
2212	8/90.22	0.42+	200	NA
2212	6/90	0.49		glass
2212	6/90_1	0.51		vvg
2212	6/90	0.56		glass
2212	8/90.21	1.16+	100-300	NA
2212	6/90	1.25		vp
2212	6/90_2	1.80		p
2212	6/90	3.23		p
2223	7/90.5	0.43+	1200	NA
2223	7/90.6	0.43+	2000	NA
2223	5/90	0.68		vvg
2223	6/90_3	0.70		vg
2223	7/90	0.71		vvg
2223	7/90	0.76		vg
2223	6/90_2	0.92		vg
2223	5/90	1.13		vg
2223	7/90.4	1.17+	500-1000	NA
2223	5/90	1.22		vg
2223	7/90	1.29		g
2223	6/90_1	1.35	800	g
2234	11/90.8	0.01+	2000	NA
2234	11/90.4	0.2+	1600	NA
2234	10/90	0.59		vvg
2234	10/90	0.63		vvg
2234	11/90	0.94		g
2234	11/90	0.99		g
2234	11/90.5	1.17+	132	NA
2234	11/90	1.4		g

2234	11/90	1.56		g
2245	NA	0.2+	100+/-50	NA
2245	NA	0.2+	300-500	NA
2245	NA	thin	100-200	NA
2245	10/90_1	0.91		p
2245	10/90_3	0.94		p
2245	10/90_2	1.41		p

The magnetization vs. temperature of the resulting glass-ceramics for four of the samples are shown in Figs. 9, 10, 11, and 12. Diamagnetism as indicated by a negative value for magnetization on this plot is confirmation of the presence of superconducting phases in the sample. The extent of diamagnetism is proportional to the volume fraction of superconducting phase. Figure 9 shows that the glass-ceramic produced from the good glass forming 2112 composition contained primarily one superconducting phase, 2212 with a Tc of 82K. As can be seen in Figs. 10, 11, and 12 glass- ceramics from the glass batches 2212, 2223, and 4334 contained the same two superconducting phases, 2212 and 2223 with superconducting transition temperatures of 110K and 85K respectively. One of the best glass formers, 4334, contained the largest concentration of the highest onset transition temperature for superconductivity (110K), see Figure 12.

DTA analysis of the quenched amorphous specimens was performed in air using heating and cooling rates of 2 degC/min. Glass transition temperatures, crystallization temperatures, melting points, etc were obtained for a number of samples. The glass transition, crystallization, and de-oxygenation temperatures were measured. There was little difference in the devitrification temperatures and de-oxygenation temperatures among the various compositions tested. The onset of devitrification was found to be around 400 ^{o}C and oxygen uptake by the devitrified material becomes significant in this same general temperature range (Minami et al, 1989[9] and Yoshimura et at, 1989[10]). But, it is only after annealing at 750 to 800 ^{o}C that these materials show evidence of the presence of one or more superconducting phases. The details of these important oxygenation and glass-ceramic crystallization studies are to be reported in a subsequent NASA TM.

In the past, some kind of anneal at high temperatures and in air or oxygen were needed to solid-state diffuse the appropriate amount of oxygen into the lattice of the BiSCCO. Little was known about this subject and the glass precursor approach offered a major step in identifying the mechanism and reason for oxygen uptake. Without the excess oxygen, superconductivity does not take place. However, the excess oxygen bubbles out when the material melts and is heated above a certain temperature. The many facets relate to the exact reasons for the oxygen uptake and loss. Chemical reasons alone indicate a temperature dependence on the oxygen concentration within the Copper oxide ad the establishment of the valence state it achieves. Physical reasons of lattice strain and bonding drive the excess oxygen concentration higher in the crystal lattice. Due to low diffusion rates, it was one thought (by Dr. Kaukler) that oxygen could be retained by a melted and oxygenated crystal long enough to quench it to a glass without significant loss of the oxygen which perhaps weakly bound to the copper ions.

This last concept prompted some experiments. TG analysis would have helped greatly to solve the problem, but these could not be done. Instead, raw weight loss and gain tests were performed. Quenched glass materials were oxygenated in a flow of oxygen at 800 C for 72 hours. Weight gains of about 3% were found, and they were predicted.

Subsequent melting for up to 15 minutes resulted in bubbling of the oxygen and some or total loss of the earlier weight gain. In one instance, a melted and quenched specimen retained a small fraction of the oxygen and formed into a glass (based on visual inspection of the fracture surfaces) even with this excess oxygen. Most cases resulted in glass formation without retained oxygen.

2112 and 2223 specimens were annealed at 500 degrees, which is well above the measured glass transition in evacuated ampoules. 2223 was run in the Perkin Elmer DSC to 500 degrees in air (at 10 degrees per minute) and was examined in the SEM and fracture surfaces were also examined. Whether 1 or 24 hours of annealing in vacuum or in air, the fracture surfaces and some SEM analysis revealed a very high fraction of glass visibly present in all these speciemens. High fractions of crystalline ceramic oxide were not visibly apparent (even under high magnification) although theoreticaly, it should have been. The reasons for these observations are not clear at this time but may figure strongly in the processing of these glasses to make superconducting ceramics.

Thermal analysis also supports these observations[11,12]. For comparison purposes, Perkin Elmer DSC 1700 data for 2112 is shown in Fig. 13. This is not DTA, but rather true DSC data where energies are plotted and not simple thermal differences. This plot can be compared to Fig. 14 which is also 2112, but this and the remaining plots to Fig. 19, are all DTA plots from the Omnitherm DTA. Figures 14 through 17 are simple DTA plots of heated as-quenched 2112, 2223, 2212 and 4334. These plots were taken in air and show features which many other researchers also showed. The features are found at around 700-850 degrees and are due to the oxygen in the air. Figures 18 and 19 show 2212 and 2112 DTA plots but without atmospheric oxygen. The air was replaced with flowing Argon (90%). Features in the earlier graphs in the range mentioned are now suppressed. Phase formation and subsequent melting of these phases has been quelled by cutting off the oxygen supply during heating through this critical temeprature range.

Summary

The results of this report show several new things about this class of oxide. They are listed below:

1. The 2112 and 4334 compositions were most easily formed into glass. Composition dependence for glass formability was confirmed.

2. These glasses had no superconducting phases present even after a low temperature anneal in a vacuum. Devitrification above the glass transition temperature does not form the phases desired. Oxygenation of the material is required to form the special phases.

3. The 4334 composition (and in second place 2112), once properly annealed in oxygen made a good superconducting material. The product had a high density due to being a cast product and not a sintered one. No attempt was made to make thin films or to obtain textured structures.

4. Normal oxygen annealing temperatures could cause some of the material to melt during the phase transformation to superconducting phases and preclude using the method of preforming the object in the glass state followed by devitrification in oxygen to make the superconducting object. Partial melting causes alteration of the form or shape and requires post anneal machining to shape the object.

5. Overheating the material past melting alsmost ensures the oxygen taken up to form the superconducting phases will be lost.

6. The best superconductors from glass precursors were shown, via magnetization measurements not to be fully composed of superconducting material. An estimate of at best 80% was made for one sample which was mostly the lower Tc phase. 4334 specimens had much of the higfher Tc phase but also some of the lower Tc phase present to dilute the crispness of the transition.

References

1. Bednorz, J.G. and K.A. Muller (1986) Z.Phys. B 64:189-193.

2. Wu, M.K., J.R. Ashburn, C.J. Torng, P.H. Hor, RlJl Meng, L.Gao, Z.J.Huang, Y.Q. Wang, and C.W. Chu (1987) Phys. Rev. Lett. 58:908.

3. Maeda, H., Y. Taraka, M. Fukutomi, and T. Asano (1988) Japan J. Appl. Phys. 27:L209.

4. Sheng, Z.Z. and A.M. Hermann (1988) Nature 332:138.

5. Hinks, D.G. (1988) Appl. Phys. Lett. 54:323.

6. Bhargave, A., R.L. Snyder, and A.K. Varshneya (1989) "Preliminary Investigations of Superconducting Glass-Ceramics in the Bi-Sr-Ca-Cu-O System" Materials Letters 8:425-431.

7. Komatsu, T., R. Sato, K. Imai, K. Matusita, and T. Yamashita (1988) "High Tc Superconducting Glass-Ceramics Based on the Bi-Sr-Ca-Cu-O System" Jap. J. Appl. Phys. 27:L550-552.

8. Tatsumisago, M., L.A. Angell, S. Tsuboi, Y. Akamatsu, N. Tohge, and T. Minami (1989) "Transition Range Viscosity of Rapidly Quenched Bi-Sr-Ca-Cu-O Glasses" Appl. Phys. Lett. 54:2268-2270.

9. Minami, T., Y. Akamatsu, M. Tatsumisago, N. Tohge, and Y. Kowada (1988) "Glass Formation of High Tc Compound BiSrCaCu2Ox by Rapid Quenching" Jap. J. Appl. Phys. 27:L777-778.

10. Yoshimura, M., T. Sung, Z. Nakagawa, and T. Nakamura (1989) "Preparation of high Tc (110K) Bi-Sr-Ca-Cu-O Superconductors from Amorphous Films by Rapid Quenching after Rapid Melting" J. Mater. Sci. Lett. 8:687-688.

11. Kaukler, W.F., T. Rolin, and E.C. Ethridge (1990) "Glass Formability in BSCCO Superconductors," presented ath the Am. Chem. Soc. SE and SW Regional Meeting, New Orleans, LA Dec. 1990.

12. Kaukler, W.F., T. Rolin, and E.C. Ethridge (1990) "Glass formation in BiSrCaCuO Superconductors" Presented at the Alabama Mater. Res. Soc. Meeting, Tuscaloosa, AL Oct. 1990.

13. Ethridge, E.C. and W. F. Kaukler (1992) NASA TM "Glass-Ceramic Processing methods for BSCCO High Temperature Superconducting Ceramics" Final Report MSFC-CDDF 90-03.

List of Figures

Figure 1. Triaxial composition diagram of the BSCCO glass-ceramic compositions investigated in this study. The two alkaline earth oxides SrO and CaO have been added together to facilitate the graphical representation.

Figure 2. The MSFC Automated Rapid Thermal Analyzer utilized for nucleation and crystallization studies on the glasses.

Figure 3. Light micrographs of polished surfaces of four as quenched glasses.

Figure 4. Quenching thermal plot for a splat quenched 2223 composition. In spite of the noisy signal caused by residual EMF effects between the molten material and the thermocouple. The quench rate is approximately 800 degC/sec.

Figure 5. Rapid splat quench of 2212 with very little thermal noise. The quench rate is 4000 degC/sec. One can see a slight inflection in the cooling curve at about 690 C. This is caused by the passage through the glass transition temperature at this temperature at the very fast cooling rate.

Figure 6. Thermal plot for a slowly quenched sample of 2212 with a quench rate of approximately 100 degC/sec. One can see an inflection on the cooling curve at about 650 degC/sec caused by the release of latent heat of fusion during the crystallization of this sample.

Figure 7. Rapid thermal analyzer quenching data from sample 2112 using the automated rapid thermal analyzer. Fig. 7a is the temperature data where as Fig. 7b is the derivative of the temperature data calibrated in degC/sec being equivalent to an uncalibrated plot of heat capacity. One can see an inflection in the cooling curve at about 780 C. This is an anomalous heat capacity effect at glass transition. Before the glass transition the cooling rate is 275 degC/sec and after the glass transition the cooling rate is 325 degC/sec. This indicates that the heat capacity of the undercooled liquid is more than the heat capacity of the glass.

Figure 8. Re-heating data from the rapid thermal analyzer for a glass sample of 2112 (8a) and the calculated delta temperature data (8b). The plot of cooling rate vs. time (temperature) is very similar to conventional DTA data. A peak indicating an increased heating rate corresponds to an exotherm (i.e. the glass crystallization peak at about 520 C. Endotherms are indicated by a decrease in the heating rate (i.e. glass transition at 460 C). Melting begins with an endotherm at about 760 C.

Figure 9. Magnetization vs. temperature for 2112 glass-ceramic. Onset of superconductivity at 76 K indicative of a single superconducting phase of 2212.

Figure 10. Magnetization vs. temperature for 2212 glass-ceramic. Onset of superconductivity at 84 K also indicative of only a single superconducting phase of 2212.

Figure 11. Magnetization vs. temperature for 2223 glass-ceramic. Two superconducting onset transitions at 105 K and 83 K indicating the presence of the two superconducting phases 2223 and 2212.

Figure 12. Magnetization vs. temperature for 4334 glass-ceramic with an initial superconducting onset temperature of 108 K and a second superconducting transition at 83 K.

Figure 13. Differential Scanning Calorimetric plot for 2112 using Perkin Elmer DSC. Peaks reveal degree of endotherm or exotherm for each phase transition.

Figure 14. First of a set of 4 DTA plots made with Omnitherm DTA. These runs were made in air and only the heating cycle is shown here. This figure is of 2112 and shows the glass transition temperature.

Figure 15. DTA plot of 2223 in air.

Figure 16. DTA plot of 2212 in air.

Figure 17. DTA plot of 4334 in air.

Figure 18. These next 2 plots are also Omnitherm DTA plots, but were run in Argon, not air. This figure is of 2212 and should be compared to Fig. 16.

Figure 19. This DTA plot in Argon is of 2112 and should be compared to Fig. 14.

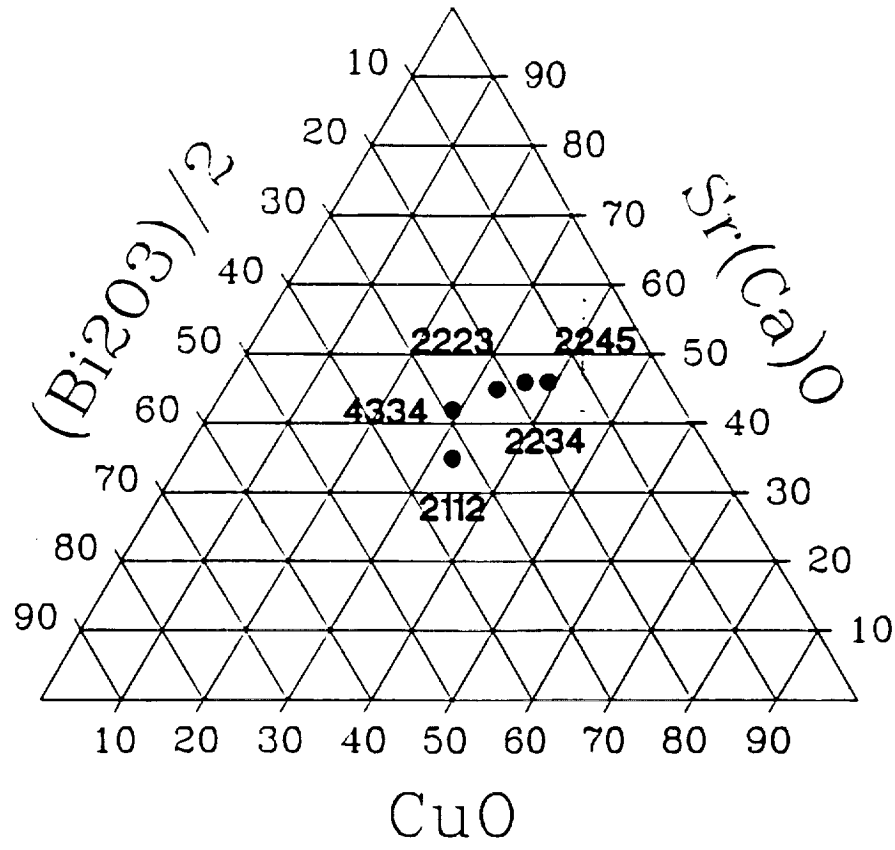

Figure 1. Triaxial composition diagram of the BSCCO glass-ceramic compositions investigated in this study. The two alkaline earth oxides SrO and CaO have been added together to facilitate the graphical representation.

Figure 2. The MSFC Automated Rapid Thermal Analyzer utilized for nucleation and crystallization studies on the glasses.

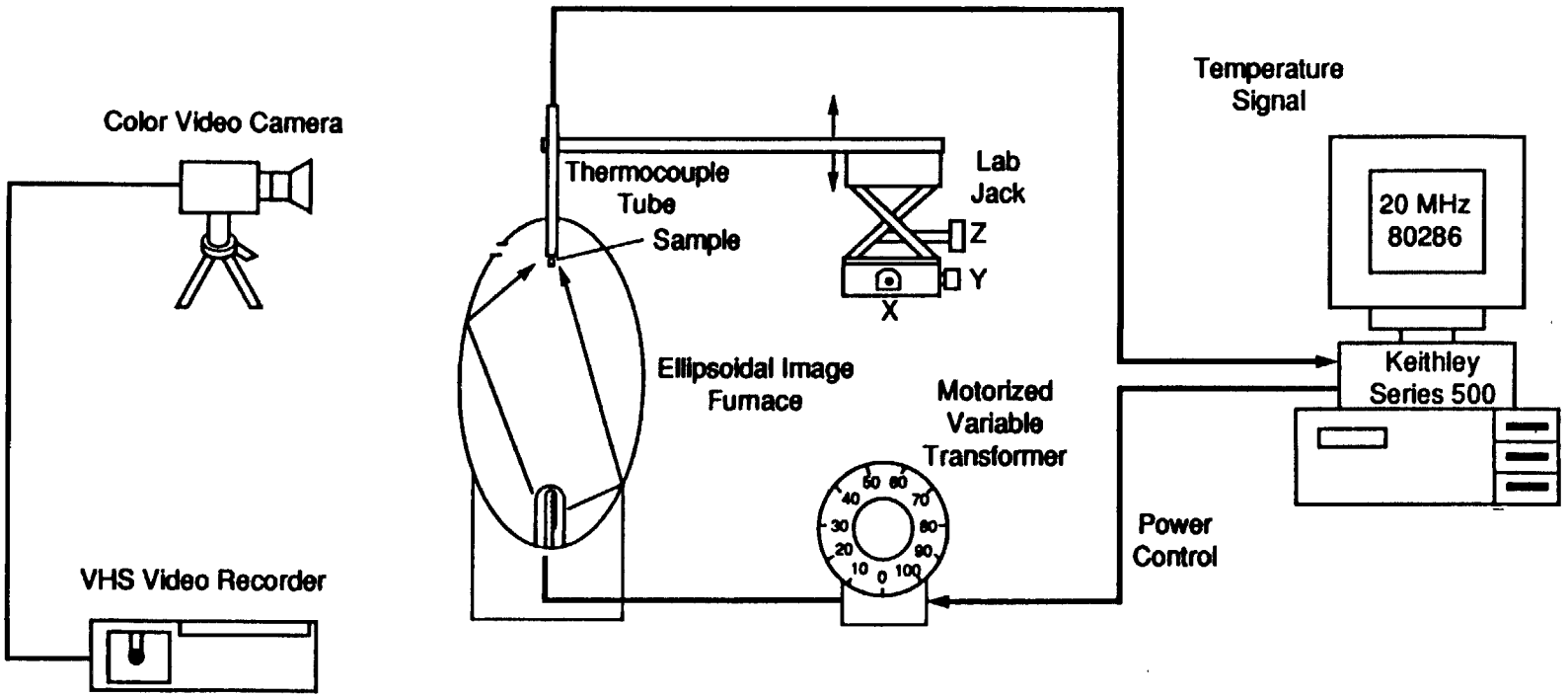

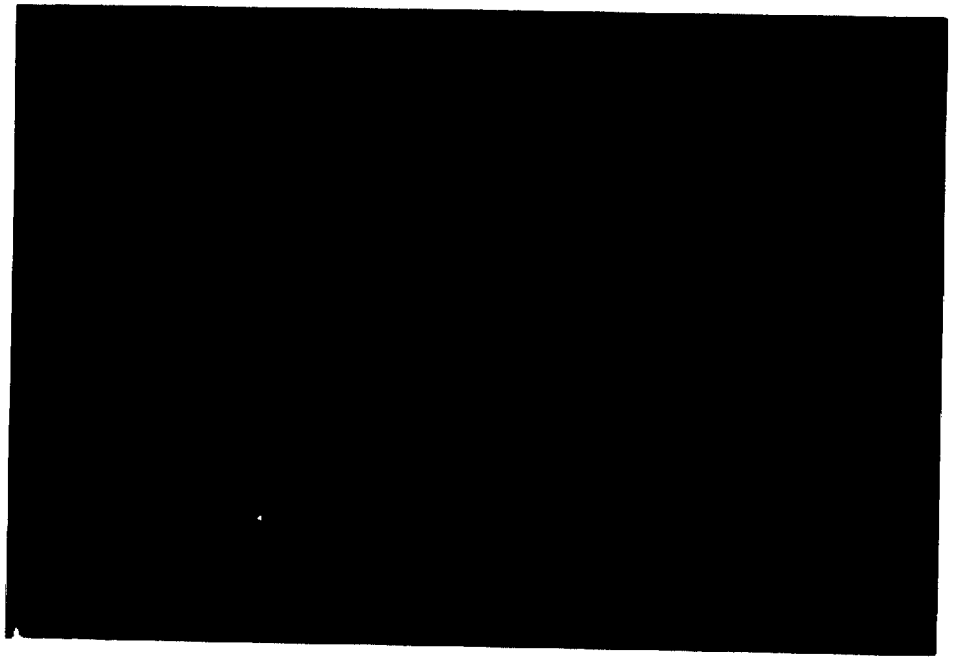

2112

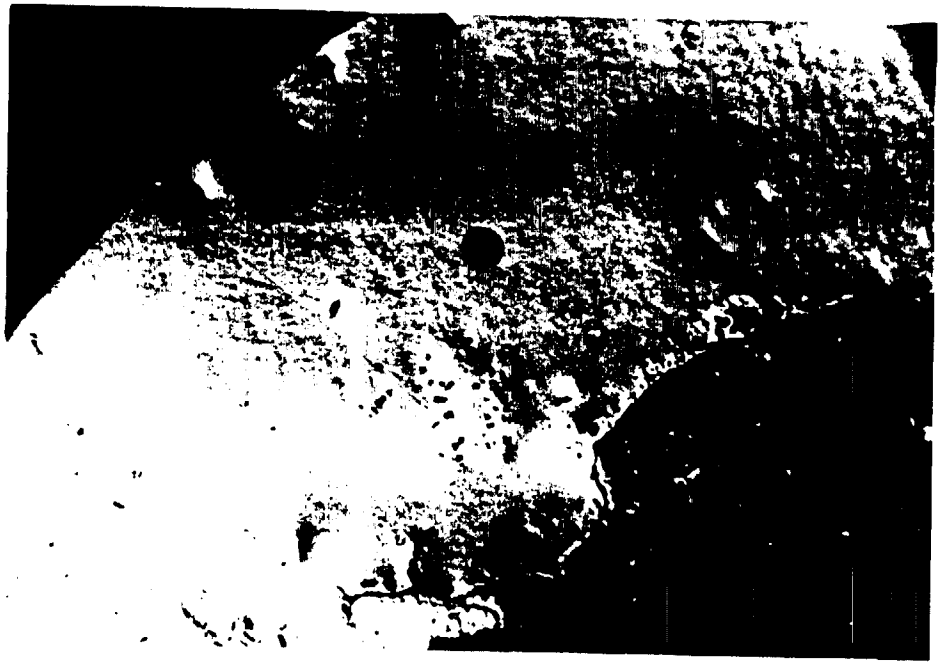

4334

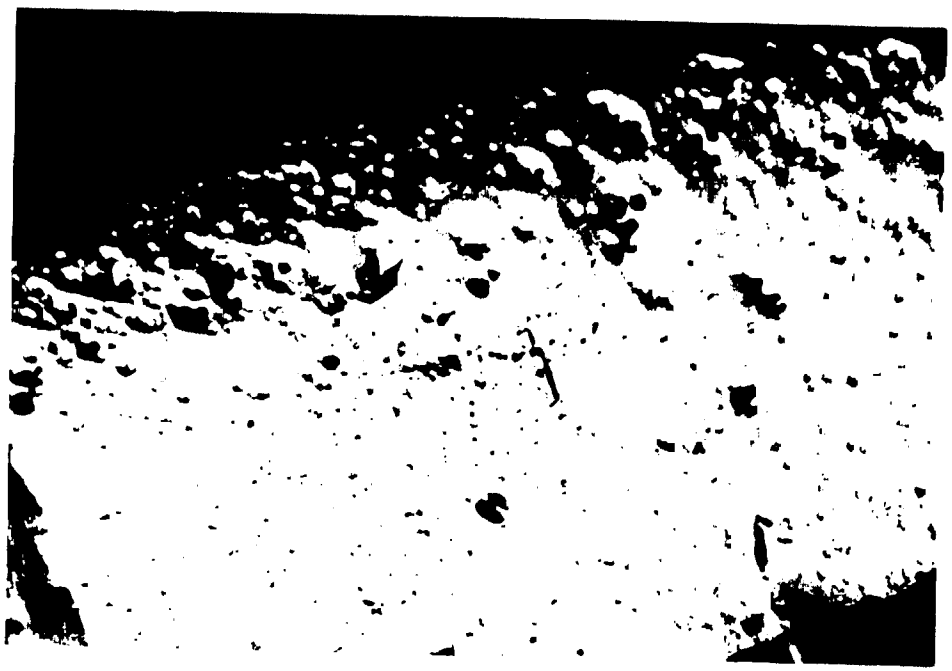

2223

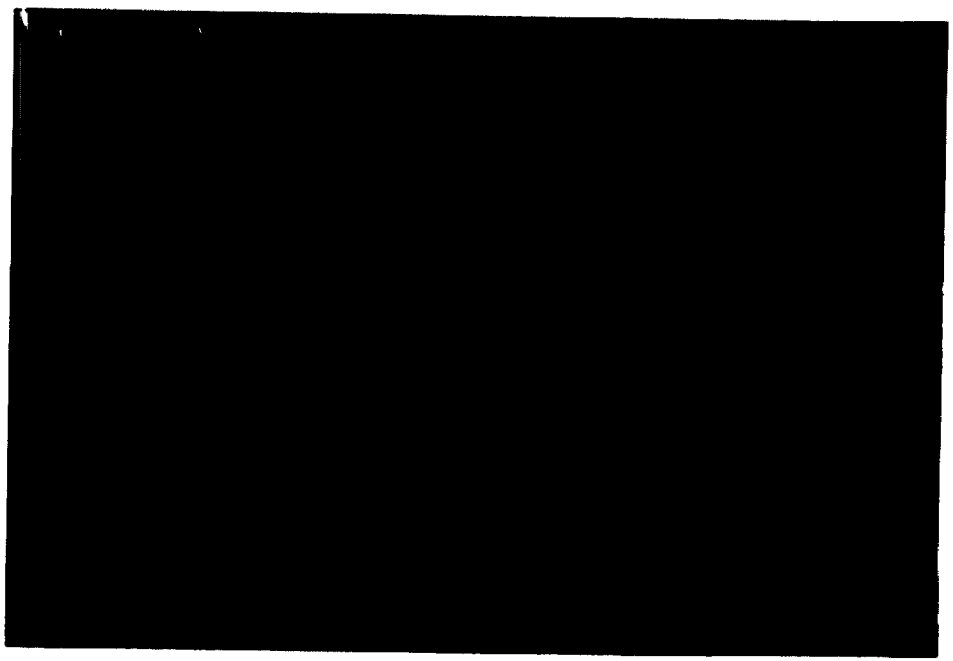

2212

Figure 3. Light micrographs of polished surfaces of four as quenched glasses.

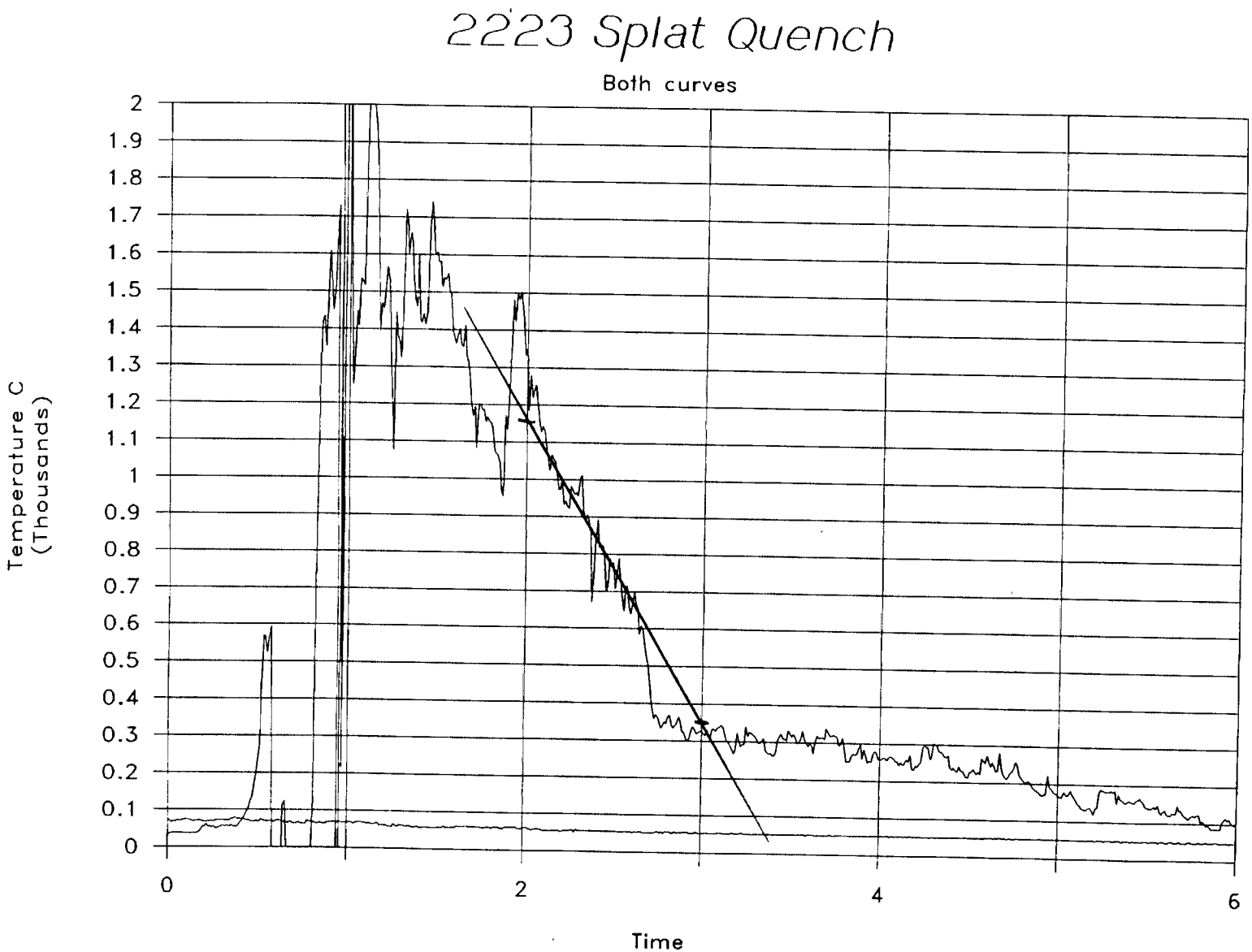

Figure 4. Quenching thermal plot for a splat quenched 2223 composition. In spite of the noisy signal caused by residual EMF effects between the molten material and the thermocouple. The quench rate is approximately 800 degC/sec.

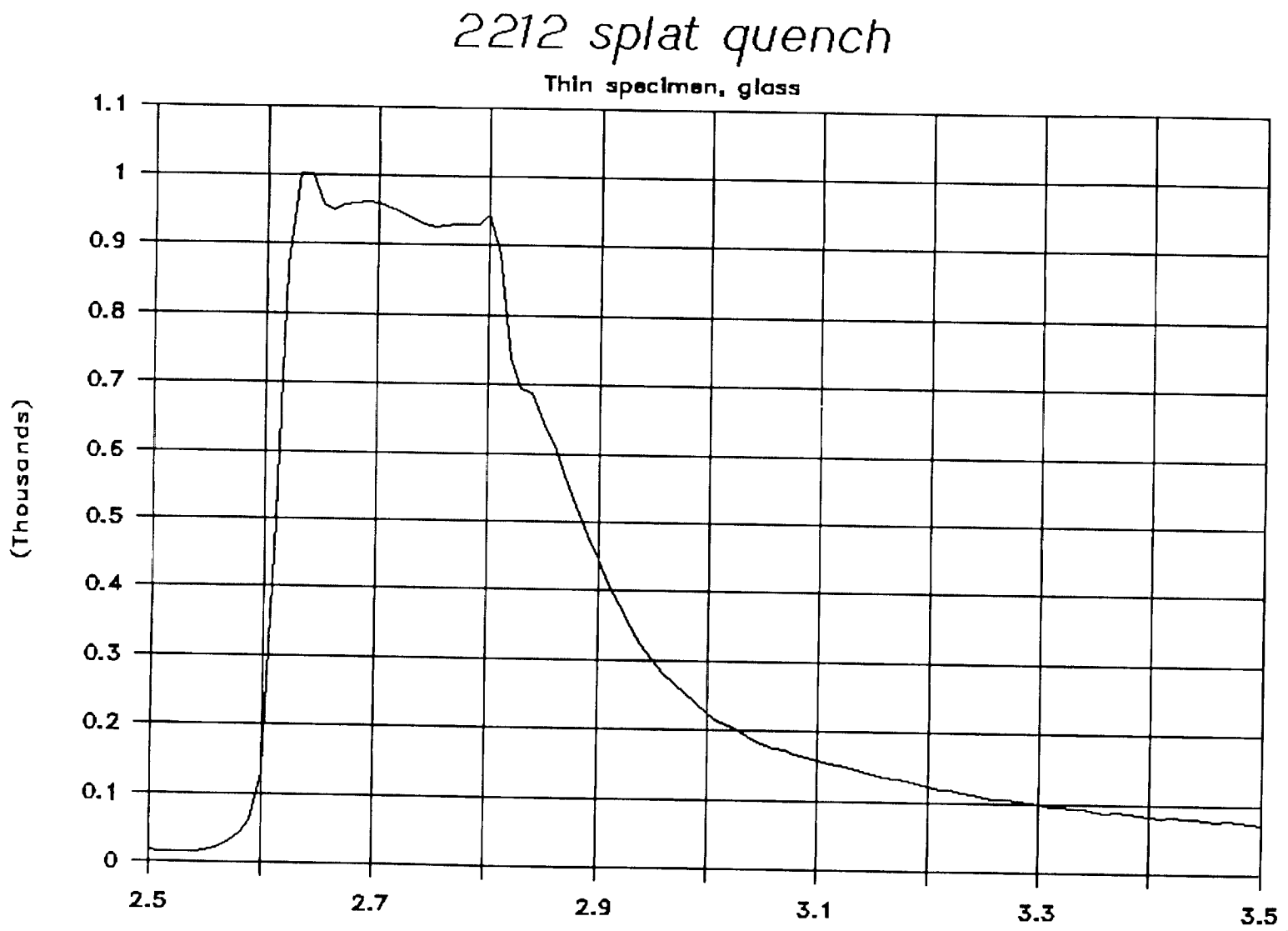

Figure 5. Rapid splat quench of 2212 with very little thermal noise. The quench rate is 4000 degC/sec. One can see a slight inflection in the cooling curve at about 690 C. This is caused by the passage through the glass transition temperature at this temperature at the very fast cooling rate.

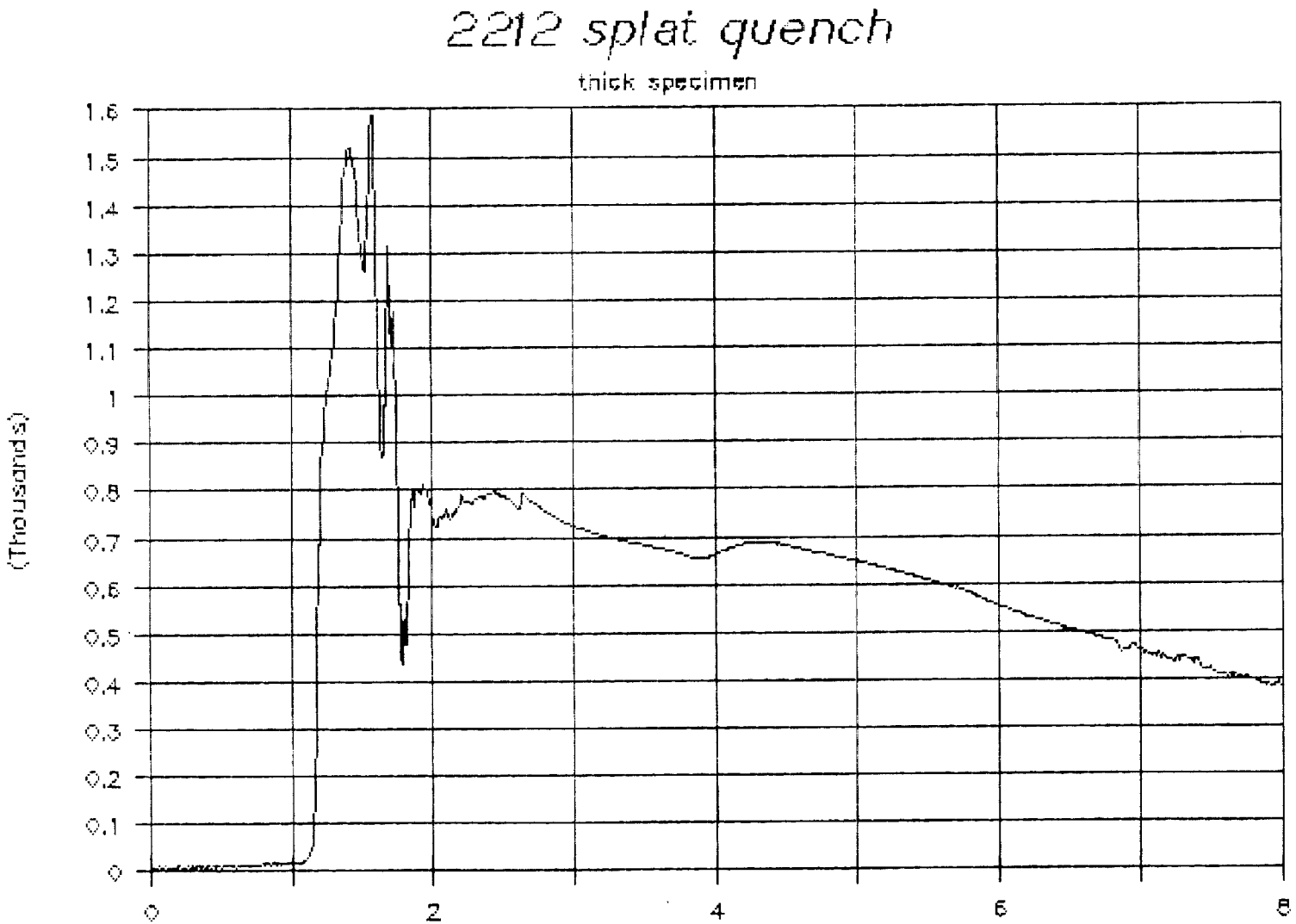

Figure 6. Thermal plot for a slowly quenched sample of 2212 with a quench rate of approximately 100 degC/sec. One can see an inflection on the cooling curve at about 650 degC/sec caused by the release of latent heat of fusion during the crystallization of this sample.

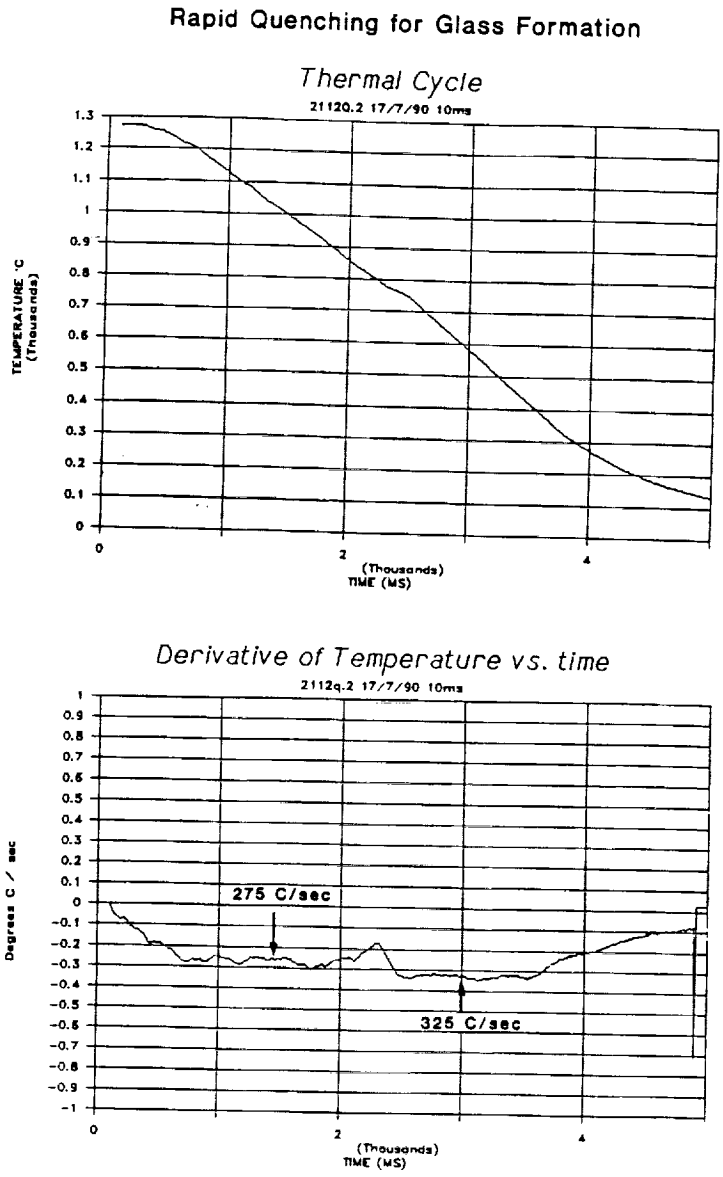

Figure 7. Rapid thermal analyzer quenching data from sample 2112 using the automated rapid thermal analyzer. Fig. 7a is the temperature data where as Fig. 7b is the derivative of the temperature data calibrated in degC/sec being equivalent to an uncalibrated plot of heat capacity. One can see an inflection in the cooling curve at about 780 C. This is an anomalous heat capacity effect at glass transition. Before the glass transition the cooling rate is 275 degC/sec and after the glass transition the cooling rate is 325 degC/sec. This indicates that the heat capacity of the undercooled liquid is more than the heat capacity of the glass.

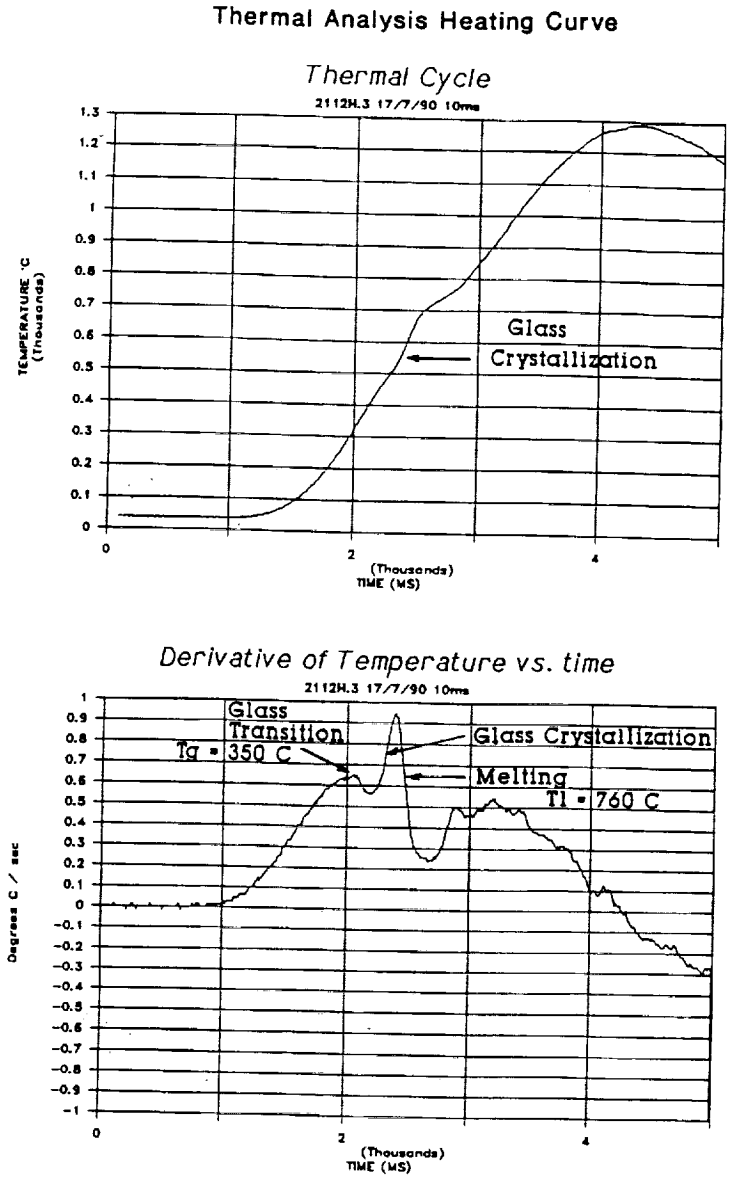

Figure 8. Re-heating data from the rapid thermal analyzer for a glass sample of 2112 (8a) and the calculated delta temperature data (8b). The plot of cooling rate vs. time (temperature) is very similar to conventional DTA data. A peak indicating an increased heating rate corresponds to an exotherm (i.e. the glass crystallization peak at about 520 C. Endotherms are indicated by a decrease in the heating rate (i.e. glass transition at 460 C). Melting begins with an endotherm at about 760 C.

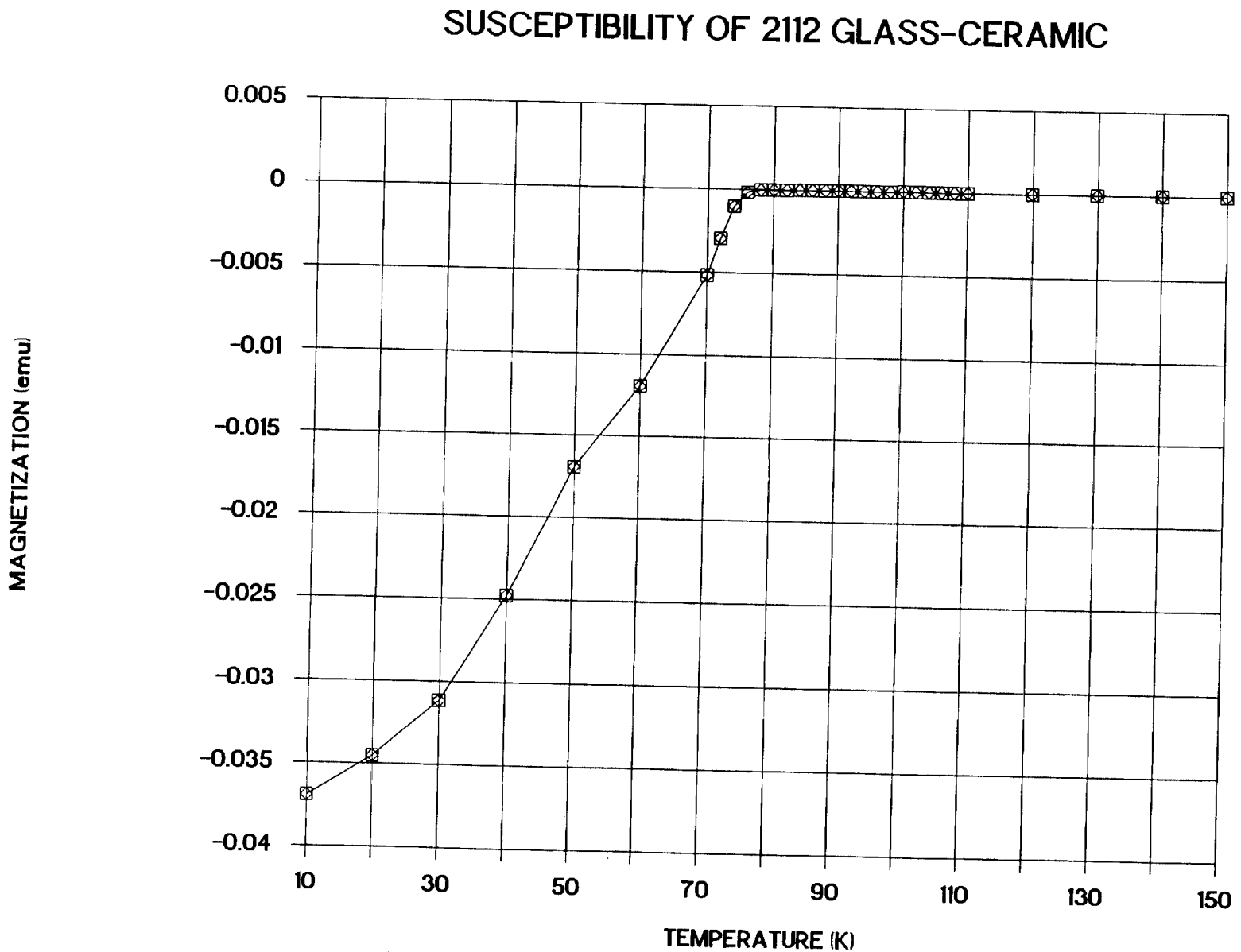

Figure 9. Magnetization vs. temperature for 2112 glass-ceramic. Onset of superconductivity at 76 K indicative of a single superconducting phase of 2212.

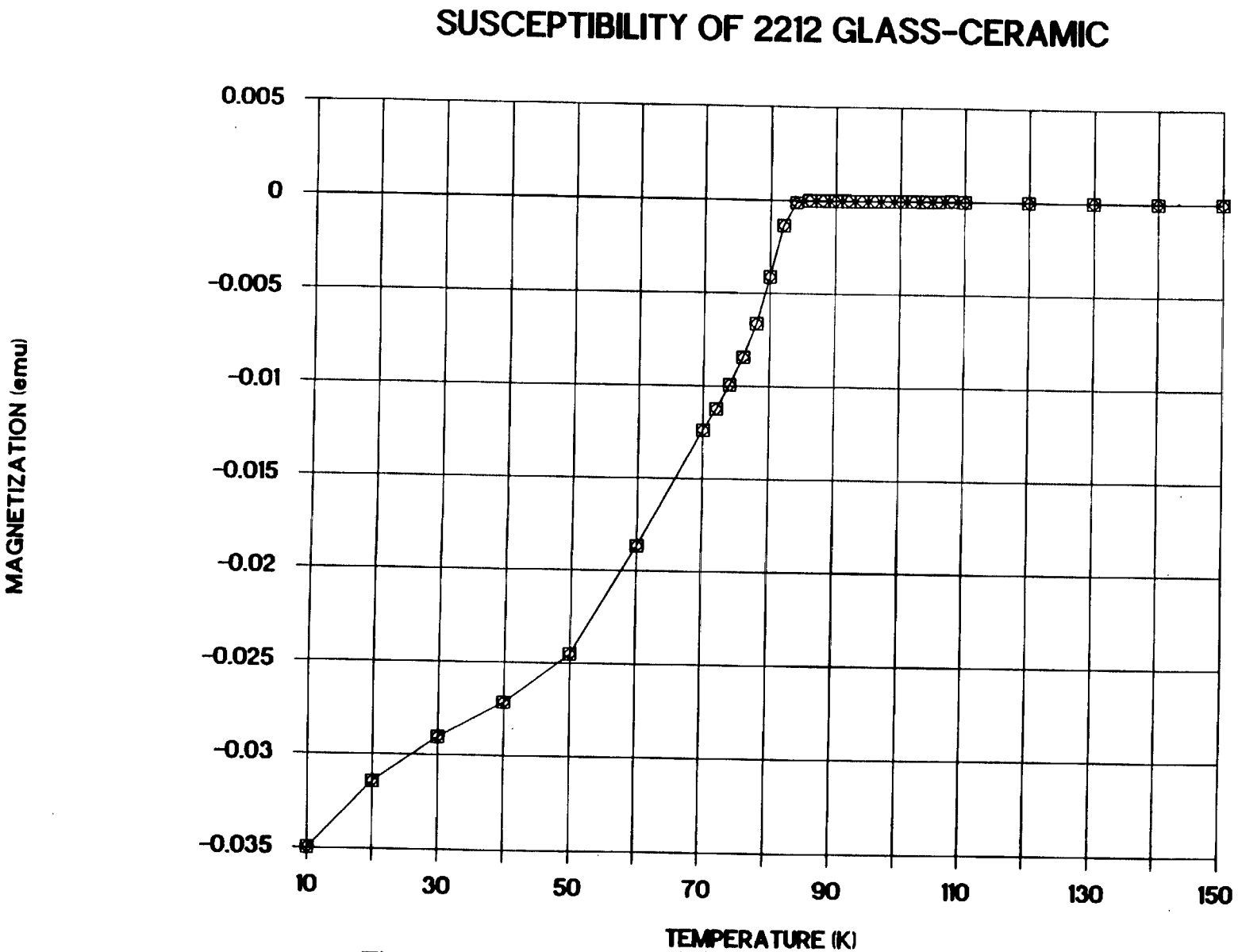

Figure 10. Magnetization vs. temperature for 2212 glass-ceramic. Onset of superconductivity at 84 K also indicative of only a single superconducting phase of 2212.

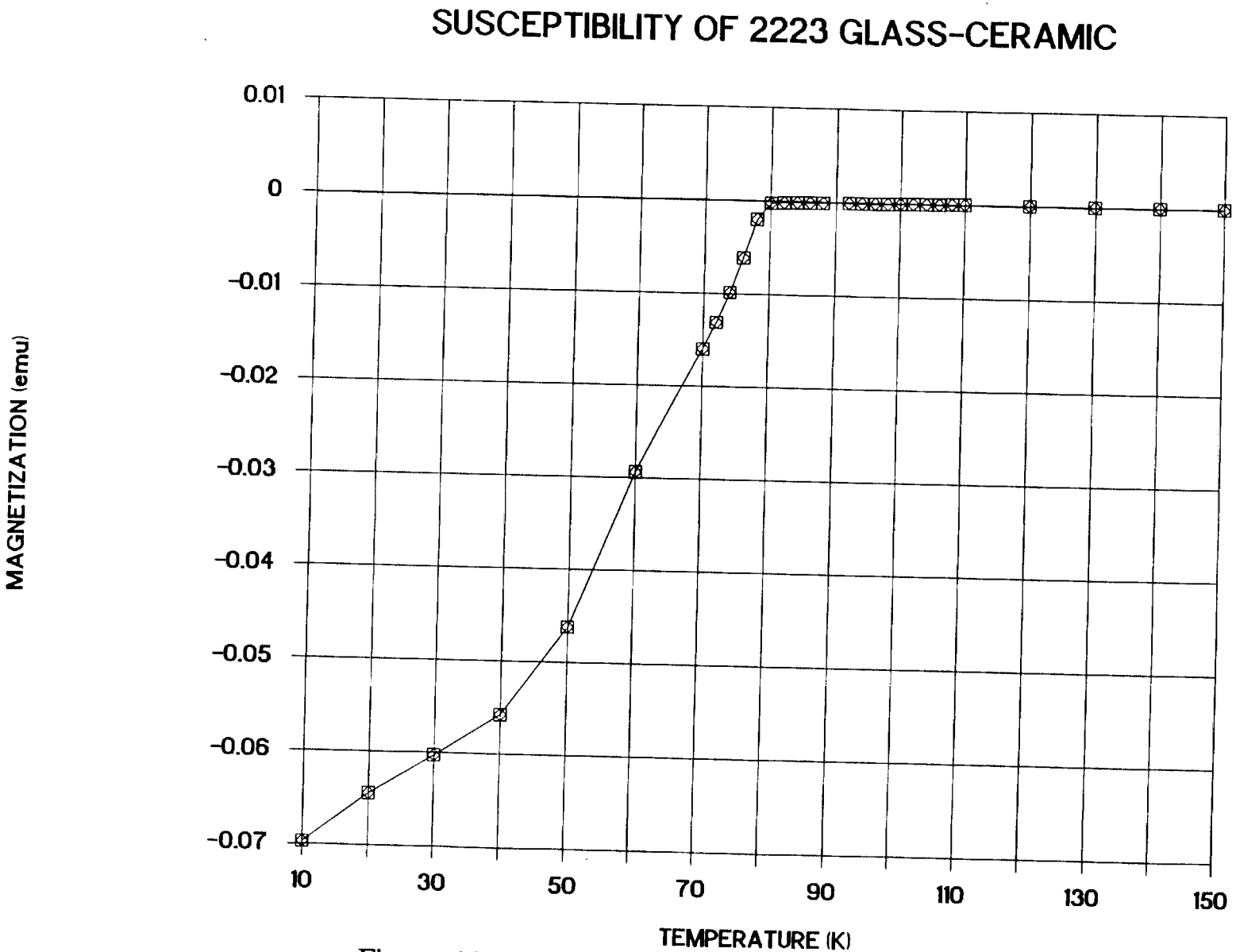

Figure 11. Magnetization vs. temperature for 2223 glass-ceramic. Two superconducting onset transitions at 105 K and 83 K indicating the presence of the two superconducting phases 2223 and 2212.

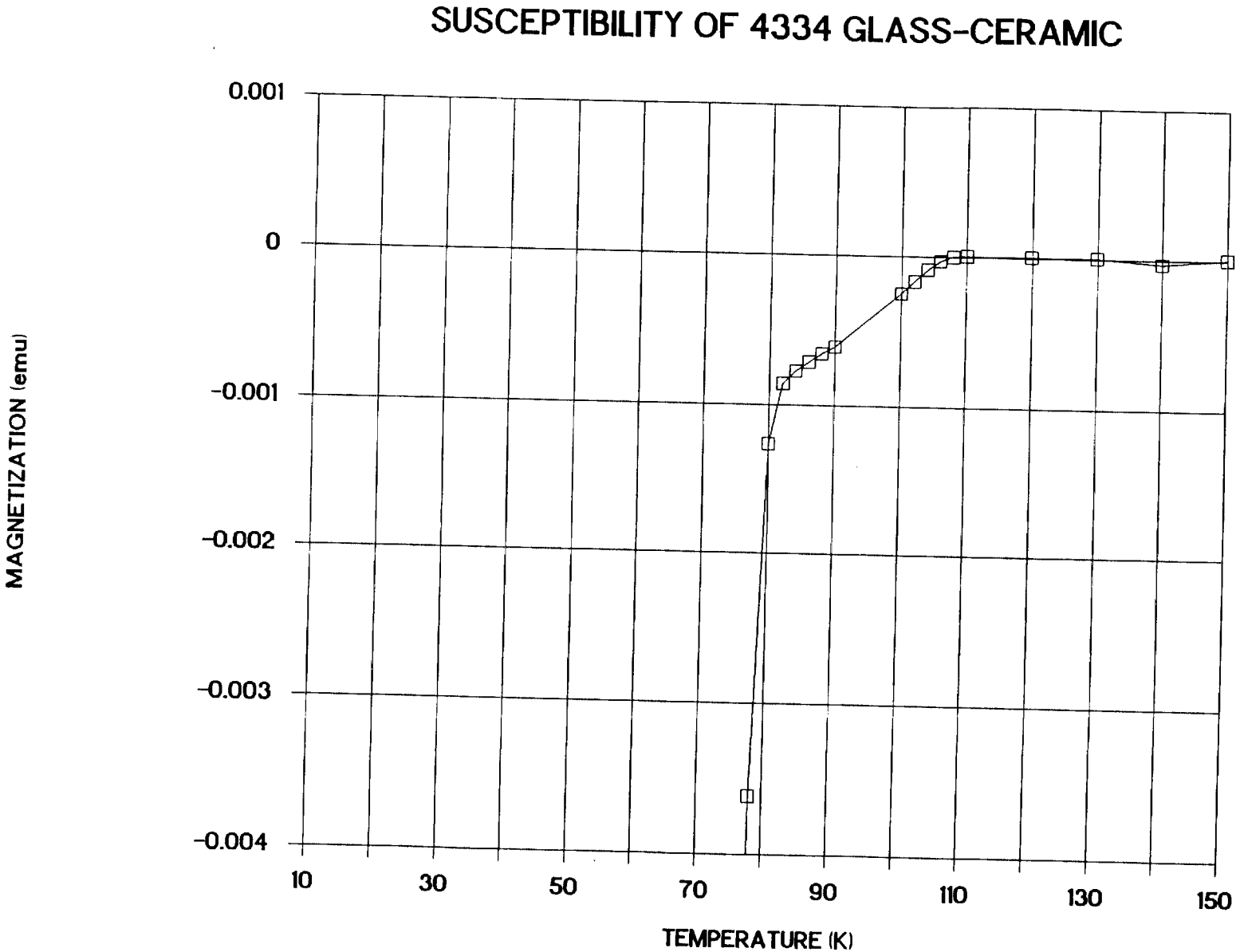

Figure 12. Magnetization vs. temperature for 4334 glass-ceramic with an initial superconducting onset temperature of 108 K and a second superconducting transition at 83 K.

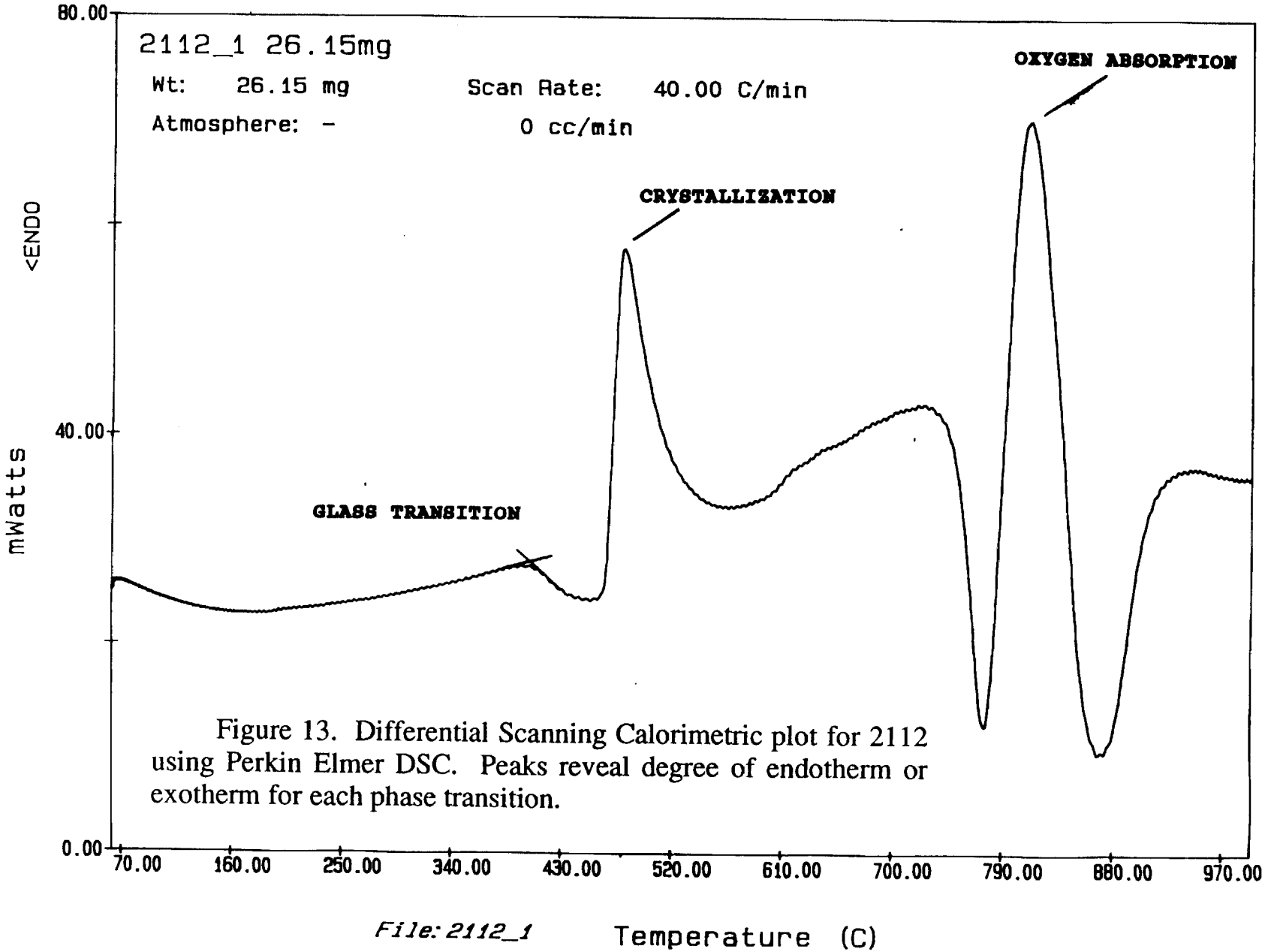

Figure 13. Differential Scanning Calorimetric plot for 2112 using Perkin Elmer DSC. Peaks reveal degree of endotherm or exotherm for each phase transition.

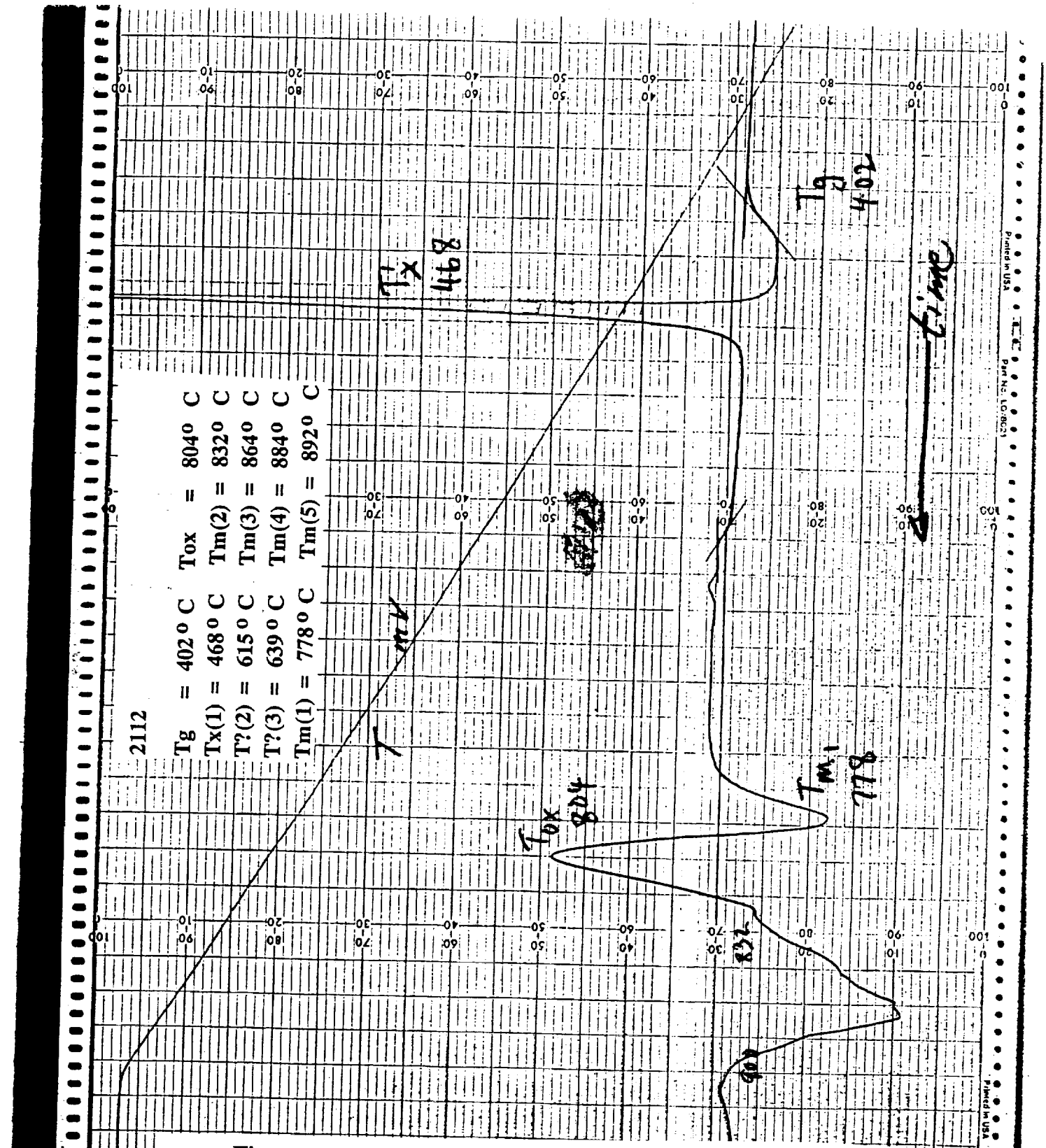

Figure 14. First of a set of 4 DTA plots made with Omnitherm DTA. These runs were made in air and only the heating cycle is shown here. This figure is of 2112 and shows the glass transition temperature.

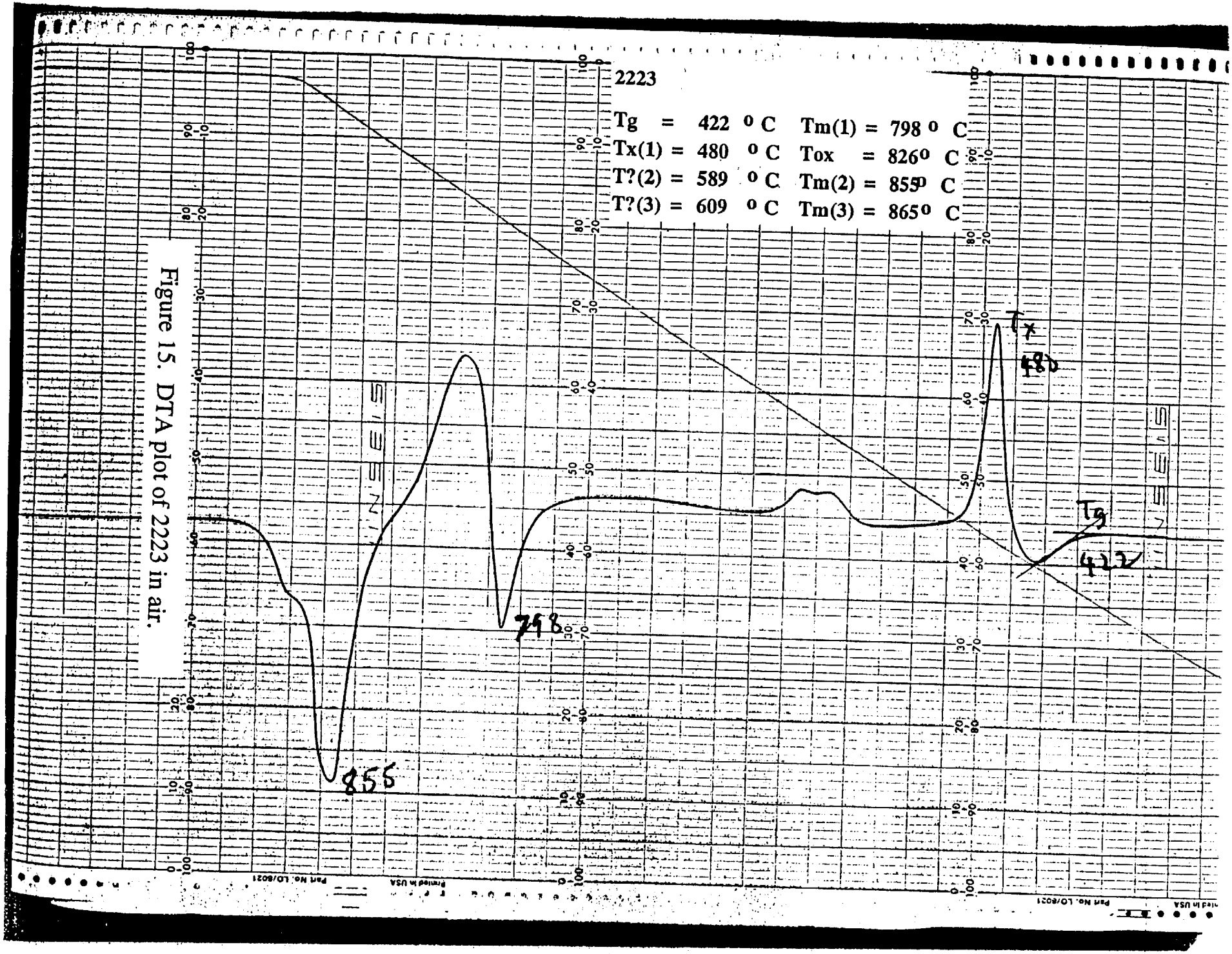

Figure 15. DTA plot of 2223 in air.

Figure 16. DTA plot of 2212 in air.

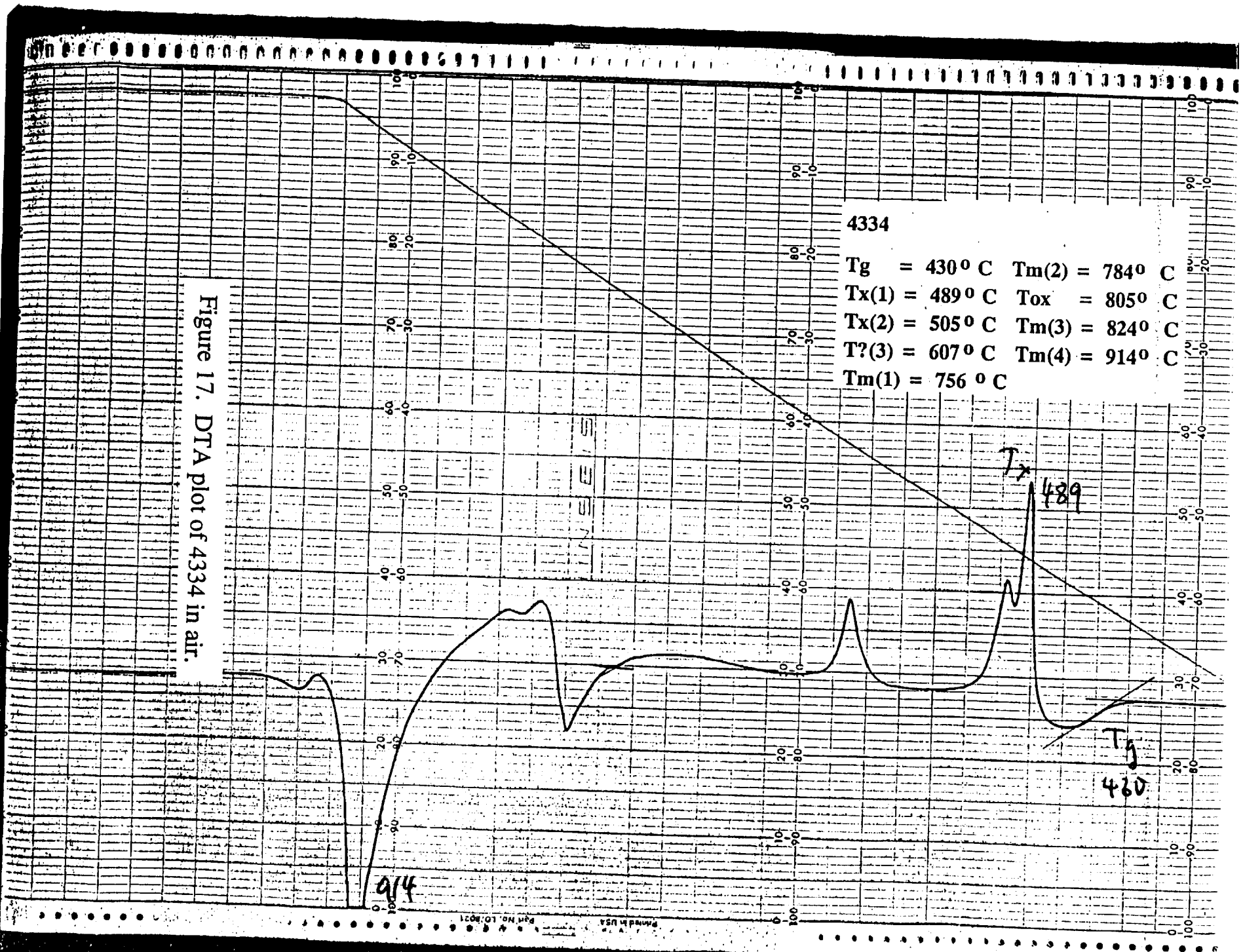

Figure 17. DTA plot of 4334 in air.

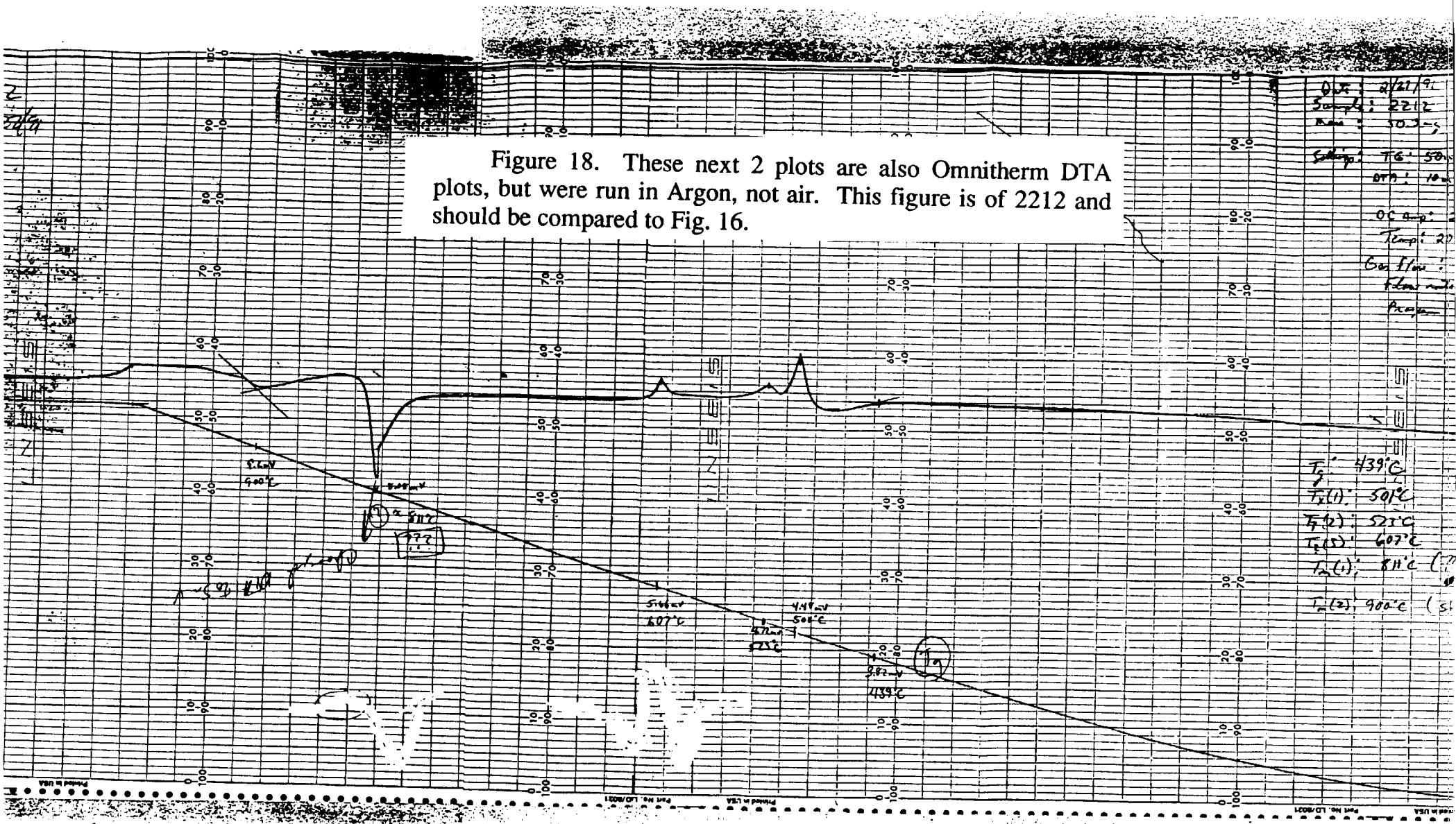

Figure 18. These next 2 plots are also Omnitherm DTA plots, but were run in Argon, not air. This figure is of 2212 and should be compared to Fig. 16.

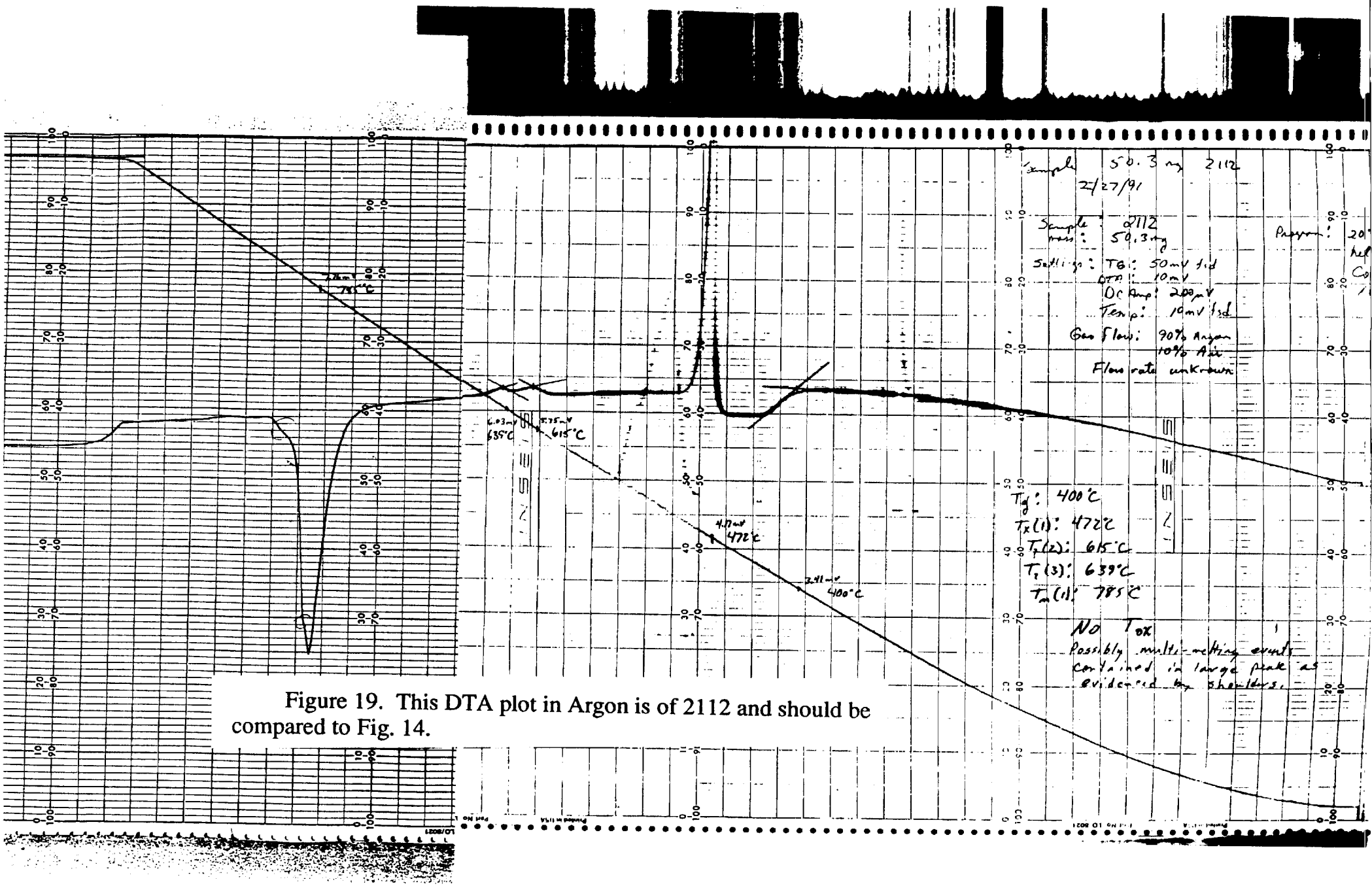

Figure 19. This DTA plot in Argon is of 2112 and should be compared to Fig. 14.